RSC Advances

ROYAL SOCIETY OF CHEMISTRY

www.rsc.org/advances

Magnetically separable Fe_3O_4-SO_3H nanoparticles as an efficient solid acid support for the facile synthesis of two types of spiroindole fused dihydropyridine derivatives under solvent free conditions

Kamalesh Debnath, Krishnadipti Singha and Animesh Pramanik*

Department of Chemistry, University of Calcutta, 92, A. P. C. Road, Kolkata-700 009, India;

Fax: +91-33-2351-9755; Tel: +91-33-2484-1647.

E-mail: animesh_in2001@yahoo.co.in

Abstract: Magnetically separable Fe_3O_4-SO_3H nanoparticles are found to act as efficient solid supported acid catalyst for the facile synthesis of two types of spiroindole fused dihydropyridine derivatives such as spiro[indolo-3,10′-indeno[1,2-*b*]quinolin]-2,4,11′-triones and indenoquinoline-spirooxindoles under solvent-free conditions. Depending upon the nature of *N*-substitutions of the starting isatins (N-H or N-R/Ar) two different types of products are formed through three component one-pot condensation reactions. Operational simplicity, reduced reaction time, lower reaction temperature, elimination of solvents, high yields of the products, easy separation of Fe_3O_4-SO_3H nanoparticles by means of an external magnetic bar and recyclability of Fe_3O_4-SO_3H nanoparticles make the present method economical, green and sustainable.

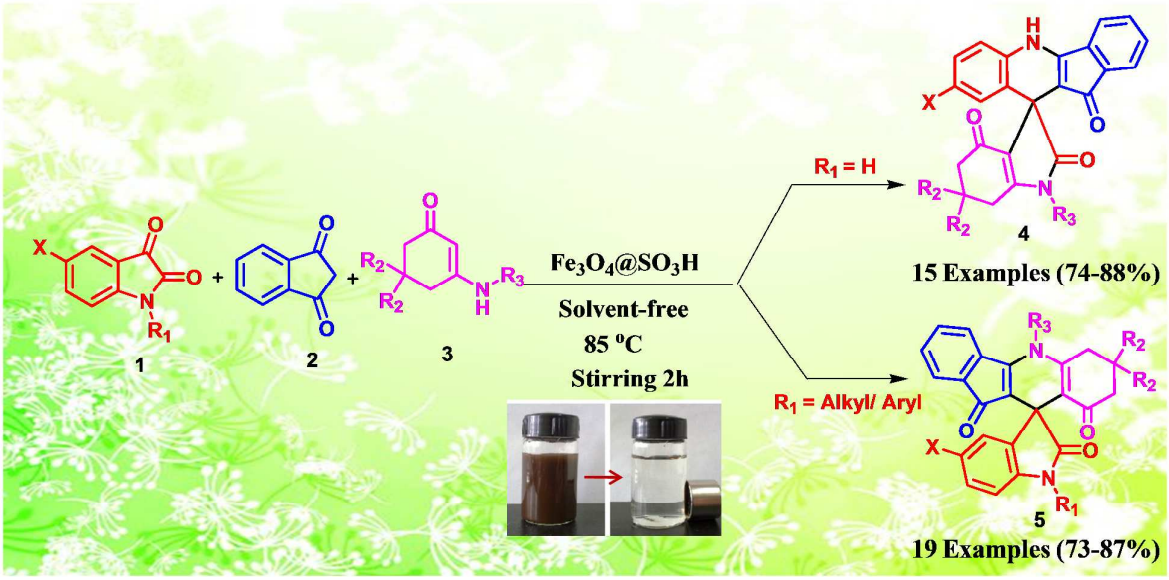

Introduction

In exploration of new green synthetic pathways, the employment of catalysts/supports with dual characteristics of homogeneous as well as heterogeneous catalyst is one of the main important aspects in contemporary chemical research. The nanocatalysts bridge the gap between these two catalytic systems by mimicking the desirable attributes of both the homogeneous and heterogeneous catalysts.[1] The main difficulty in the nanocatalyst mediated organic reactions is the separation and recovery of the catalyst through conventional filtration as it blocks the pores and valves of the filter papers. Because of their insolubility and paramagnetic nature, the magnetically separable nanoparticles (MSNPs) can easily be separated and isolated from the reaction mixtures by means of an external magnet. In this sense, development of novel reagents and magnetically retrievable nano-particles leaves immense significance for the environmentally benevolent synthesis of biologically important heterocycles. In this regard, nano-magnetite Fe_3O_4-SO_3H emerges as an efficient and sustainable acid catalyst for various organic reactions.[2]

The recent researches in organic chemistry revolve around designing of economical syntheses in order to save chemical resources and to prevent the chemical impact on

environment. To achieve these desirable syntheses, chemists are interested in multicomponent reactions (MCR) since they have become a significant part of today's arsenal of methods in combinatorial chemistry due to their valued features such as atom-economy, straightforward reaction design, and the opportunity to construct target compounds by the introduction of several diversified elements in a single chemical event.[3] Compounds with spiro skeletons not only constitute subunits in numerous alkaloids, but are also the templates for drug discovery and scaffolds for combinatorial libraries.[4] The spiro-fused cyclic frameworks are the core of many natural products with various types of bioactivities such as progesterone receptor modulators,[5] anti-HIV,[6] anticancer,[7] antitubercular,[8] antimalarial,[9] and MDM2 inhibitor.[10] On the basis of the above reports and also as a part of our research interest in developing efficient and environmentally benign synthetic methodologies,[11] herein, we wish to report a greener methodology for one-pot three-component synthesis of spiro[indolo-3,10′-indeno[1,2-*b*]quinolin]-2,4,11′-triones (**4**) using isatin (**1**), indane-1,3-dione (**2**) and enamines (**3**) in the presence of nano-magnetite Fe_3O_4-SO_3H under solvent-free condition (Scheme 1). Interestingly, when we choose *N*-substitued isatins in place of isatin, we obtained completely different products such as indenoquinoline-spirooxindoles (**5**) instead of spiro[indolo-3,10′-indeno[1,2-*b*]quinolin]-2,4,11′-triones (**4**) under the same reaction conditions (Scheme 1).

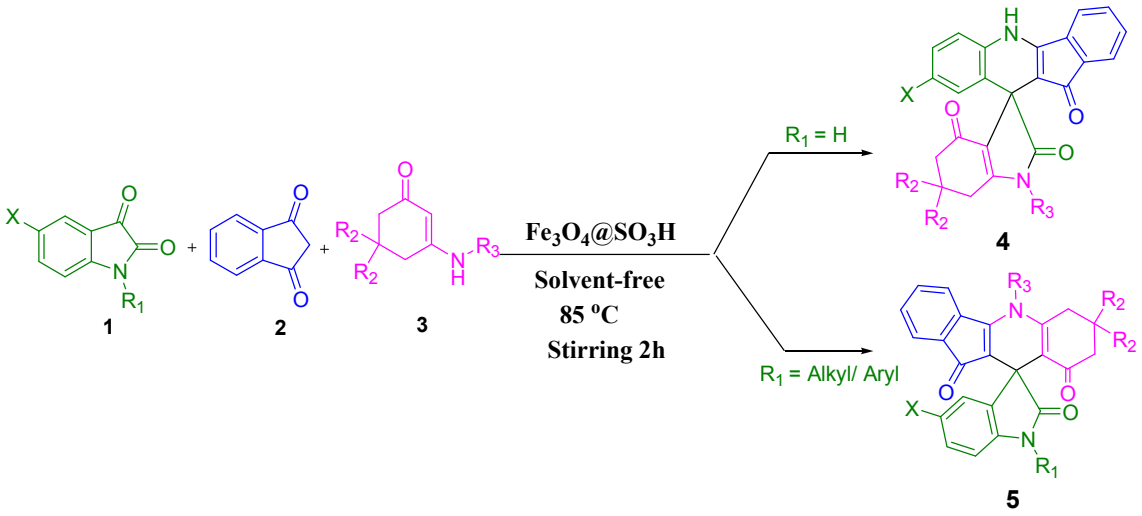

Scheme 1: Synthesis of spiro[indolo-3,10′-indeno[1,2-*b*]quinolin]-2,4,11′-triones (**4**) and indenoquinoline-spirooxindole derivatives (**5**)

Results and discussion

During our initial studies towards the development of Fe_3O_4-SO_3H as nano-magnetic solid support for the one pot three component synthesis of spiro[indolo-3,10′-indeno[1,2-*b*]quinolin]-2,4,11′-triones (**4**) under solvent-free conditions, we attempted to optimize the reaction conditions taking isatin (**1**), indane-1,3-dione (**2**) and 3-butylamino-5,5-dimethyl-cyclohex-2-enone (**3**) in 1:1:1 molar proportion (Scheme 2). In this process various parameters such as the effect of catalysts, solid supports, temperature and solvents at different experimental conditions were investigated (Table 1). The results of the optimization studies are summarized in Table 1. Initially, we attempted to carry out the three component reaction in EtOH, using several Brønsted and Lewis acid catalysts such as conc. H_2SO_4, formic acid, lactic acid, *p*-TSA, $FeCl_3$ and silica sulphuric acid (SSA) under refluxing condition for different period of time (10-4 h) (Table 1, entries 1-7). Low to moderate yields of the product **4a** were obtained in all these reactions. Interestingly significant reduction of reaction time (2 h) with an improved yield of **4a** (~70%) was observed when silica sulfuric acid (SSA) was

used as the solid support under solvent free condition (Table 1, entry 8). This result incited us to carry out the optimization study in presence of various solid supports such as nano-Fe_3O_4, melamine sulfonic acid (MSA) and acid-surfactant combined catalyst PEG-OSO_3H, under solvent-free condition at 85ºC (Table 1, entries 9-11). In all cases the yield of the desired product was moderate. Gratifyingly, high yield of product **4a** (~85%) was obtained when the substrates were allowed to react on the solid surface of magnetically retrievable nano Fe_3O_4-SO_3H for 2h at 85ºC under solvent-free conditions with continuous stirring (Table 1, entry 12). It is envisioned that, the adsorption of the reactant molecules on the large surface area of the nano particles increases the local concentration around the active sites of Fe_3O_4-SO_3H and accelerates the reaction rate significantly. Then we carry out the optimization study to examine the influence of the stoichiometry of nano Fe_3O_4-SO_3H (300 mg-1.0 g) at different temperatures (ambient temp. to 100 ºC) for the best yield of **4a** (Table 1, entries 12-18). The study revealed that best yield of the product **4a** was obtained when the substrates **1**, **2** and **3** taking 1 mmol each were allowed to react on the solid surface of nano Fe_3O_4-SO_3H (500 mg) at 85 ºC under solvent-free condition. The optimized methodology tolerates a wide spectrum of isatins and enamines with good to excellent yields of the targeted molecules (Table 2). Our present methodology is more advantageous than the previously reported methodology[12] in many respects such as eradication of solvent, reduction of reaction time (from 5 h to 2 h), lowering of reaction temperature and simple work-up procedure due to easy separation of the nano particles by magnet and successive recyclability of the solid support. Refluxing of the three substrates **1**, **2** and **3** in water as seen in the previously reported method[12] is energetically very expensive due to high heat capacity of water. The formation of the final products in the present method was confirmed by IR, ^{1}H NMR, ^{13}C NMR spectroscopy, elemental analysis and also by matching the melting points of some of the compounds with the reported values.[12] The X-ray crystal structure of products **4a** is presented in Figure 1.

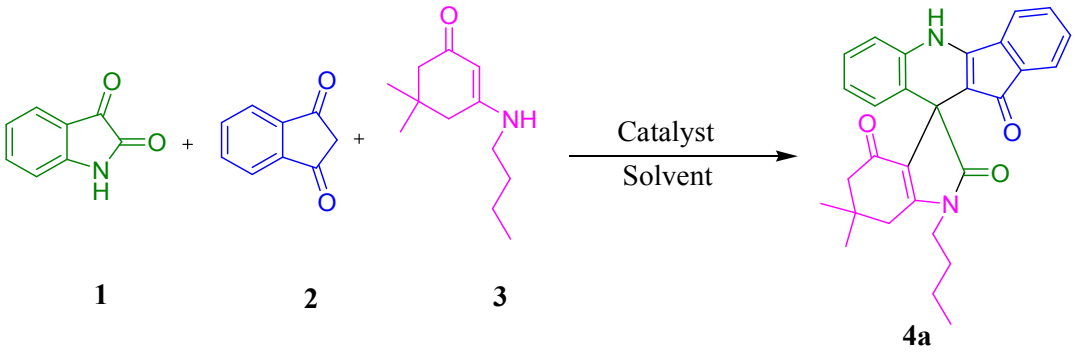

Scheme 2: Optimization of the reaction conditions.

Table 1: Optimization of reaction conditions for the synthesis of **4a**

Entry	Solvent (10 ml)	Catalyst/ Solid Support	Load	Time (h)	Temp.	Yield[a] (%)
1	EtOH	H_2SO_4	20 mol%	1	Reflux	Trace
2	EtOH	L-proline	20 mol%	10	Reflux	Trace
3	EtOH	Formic acid	20 mol%	14	Reflux	55
4	EtOH	Lactic acid	20 mol%	14	Reflux	58
5	EtOH	*p*-TSA	20 mol%	10	Reflux	53
6	CH_3CN	$FeCl_3$	20 mol%	24	Reflux	37
7	EtOH	Silica sulphuric acid (SSA)	20 mol %	4	Reflux	61
8	—	SSA	500 mg	2	85ºC	70
9	—	Nano- Fe_3O_4	500 mg	24	85ºC	Trace
10	—	PEG-OSO_3H	500 mg	12	85ºC	60
11	—	Melamine sulfonic acid (MSA)	500 mg	12	85ºC	45
12	**—**	**Fe_3O_4-SO_3H**	**500 mg**	**2**	**85ºC**	**85**
13	—	Fe_3O_4-SO_3H	300 mg	2	85ºC	80
14	—	Fe_3O_4-SO_3H	800 mg	2	85ºC	85
15	—	Fe_3O_4-SO_3H	1.0 g	2	85ºC	85
16	—	Fe_3O_4-SO_3H	500 mg	12	r.t.	Trace
17	—	Fe_3O_4-SO_3H	500 mg	6	70ºC	78
18	—	Fe_3O_4-SO_3H	500 mg	2	100ºC	85

[a]Isolated Yields.

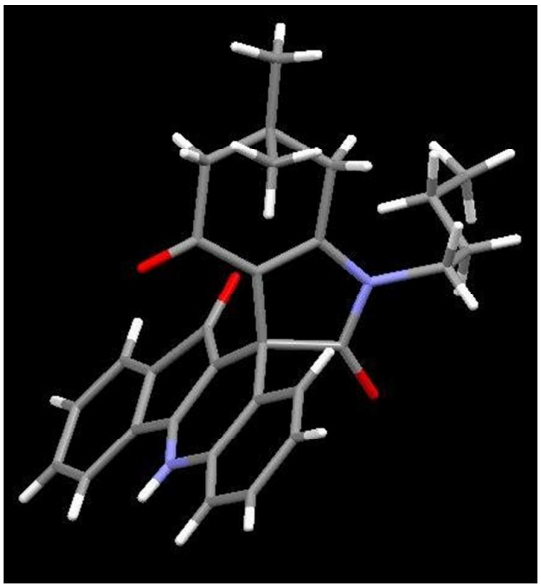

Figure 1. Crystal structure of compound **4a**. Color code: red, oxygen; blue, nitrogen; grey, carbon; white, hydrogen (CCDC 1042541).†

Table 2: Library synthesis of spiro[indolo-3,10′-indeno[1,2-*b*]quinolin]-2,4,11′-triones compounds **4a-o**[a]

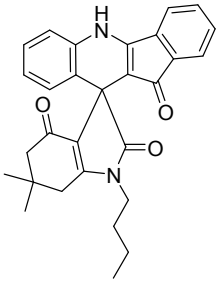 **4a (85%)**	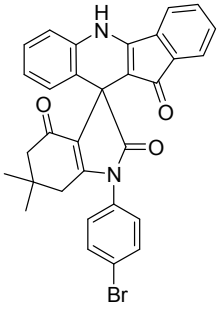 **4b (80%)**	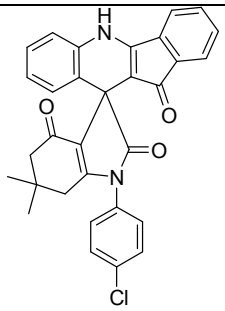 **4c (81%)**	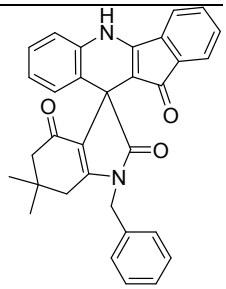 **4d (79%)**
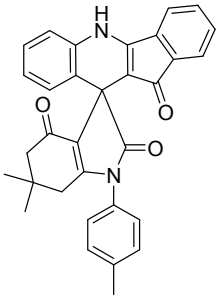 **4e (88%)**	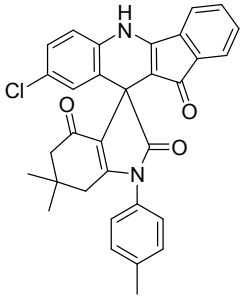 **4f (76%)**	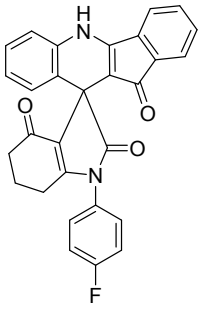 **4g (78%)**	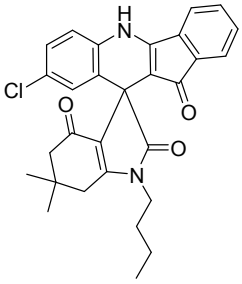 **4h (87%)**
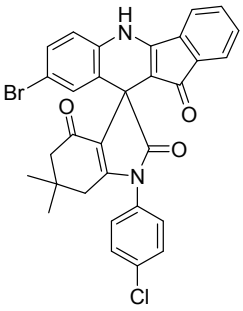 **4i (75%)**	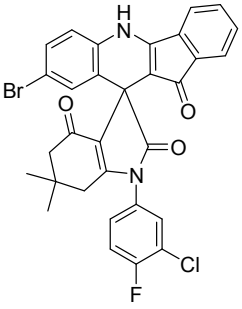 **4j (74%)**	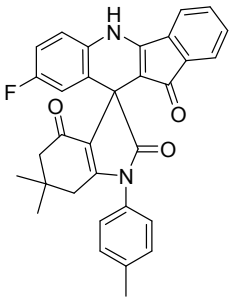 **4k (74%)**	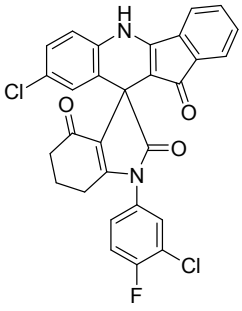 **4l (78%)**
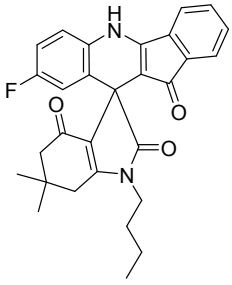 **4m (82%)**	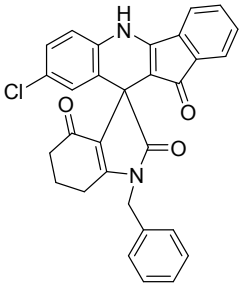 **4n (85%)**	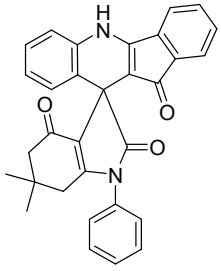 **4o (86%)**	

[a]Isolated Yields

Next we attempted to evaluate the scope and generality of this reaction by employing *N*-ethyl isatin (**1**), an *N*-substituted isatin, in place of isatin along with indane-1,3-dione (**2**) and 3-butylamino-5,5-dimethyl-cyclohex-2-enone (**3**). Surprisingly the crystal structure elucidation of the product shows that it is not of type **4** as seen previously, but a different isomeric spiro derivative **5a** (Figure 2). The formation of different products such as **4** and **5** depending upon the nature of *N*-substitution of isatins was not correctly established by Yang *et al*.[13] This new and interesting result motivates us to synthesis a new series of indenoquinoline-spirooxindoles **5a-s** employing various *N*-alkyl and *N*-aryl substituted isatins (Table 3).

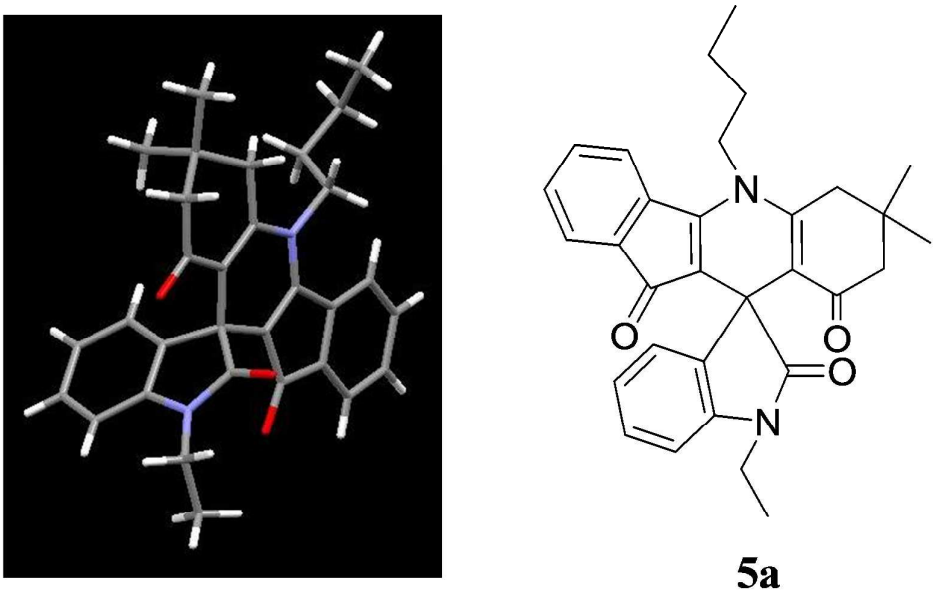

Figure 2. Crystal structure of compound **5a**. Color code: red, oxygen; blue, nitrogen; grey, carbon; white, hydrogen (CCDC 1042534).†

Table 3: Library synthesis of indenoquinoline–spirooxindole compounds **5a-s**[a]

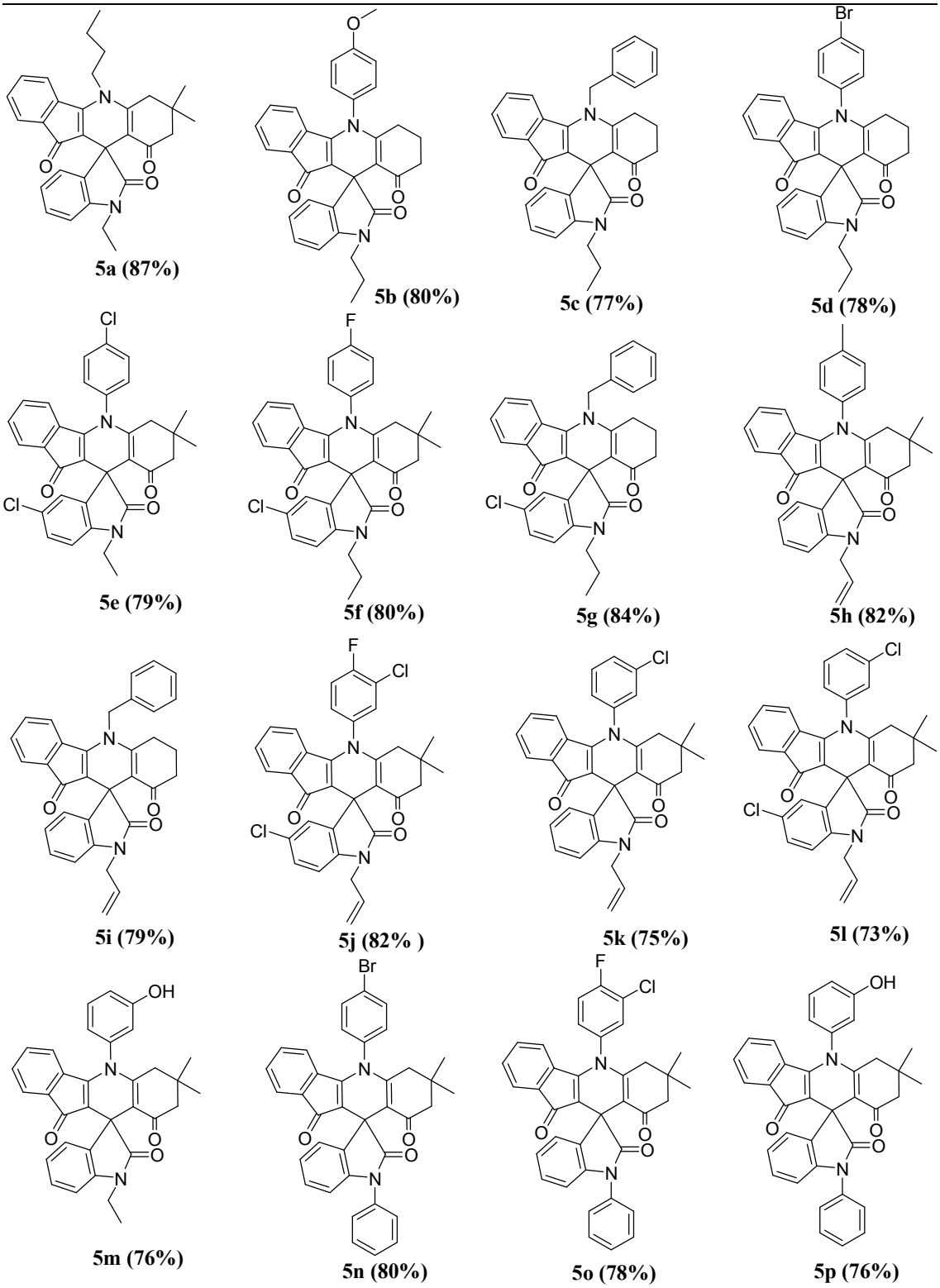

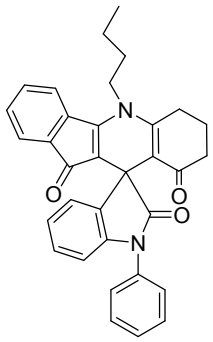

5q (79%)

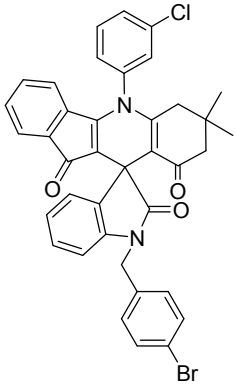

5r (83%)

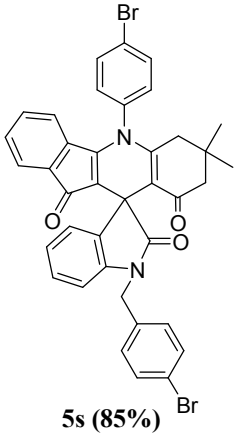

5s (85%)

[a]Isolated Yields.

Elemental analyses of the as-synthesized nano-particles were performed at EDX equipped onto TEM. The sulphur peak in the quantitative EDX analysis of prepared Fe_3O_4-SO_3H indicates the incorporation of the -SO_3H group on the surface of the solid support due to the reaction between Fe_3O_4 NPs with chlorosulfonic acid (Fig. 3a). Field emission scanning electron microscopic (FE-SEM) images were taken at the operating voltage of 5.0 kV to elucidate the morphology of the synthesized Fe_3O_4-SO_3H nanoparticles (Fig. 3b). It is clearly evident from the image in Fig. 3b that the spherical shaped nanocat-Fe_3O_4-SO_3H nanoparticles have diameter within the range of ~23 to ~43 nm. It is interesting to note that, the nano-particles exhibit a marked tendency to form clusters, may be due to the weak intermolecular hydrogen bonding between the -SO_3H groups of Fe_3O_4-SO_3H.

The morphology and microstructure of Fe_3O_4-SO_3H nanoparticles were investigated by high-resolution transmission electron microscopy (HRTEM) at an accelerating voltage of 200 kV (Fig. 3c and 3d). The analysis of Fig. 3c clearly shows the uniform formation of almost spherically shaped Fe_3O_4-SO_3H nanoparticles with a narrow distribution of size within the range of ~14 to ~23 nm. The characterization of the nano-Fe_3O_4-SO_3H by TEM images, before (Fig. 3c) and after five times applications (Fig. 3d) shows the unaltered particle size.

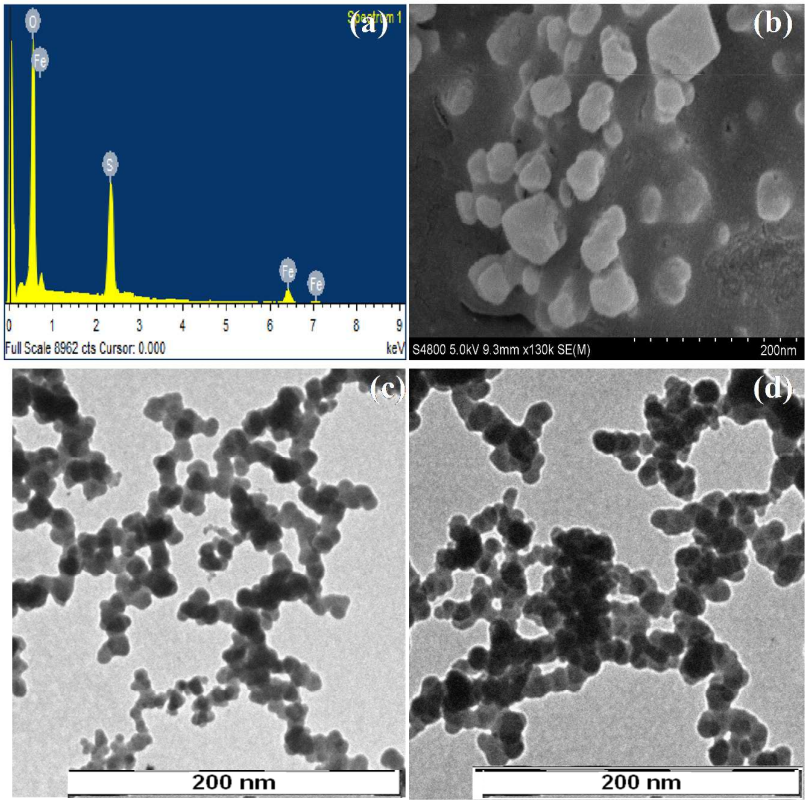

Figure 3. (a) TEM-EDX of Fe_3O_4-SO_3H MNPs; (b) SEM image of Fe_3O_4-SO_3H MNPs; and TEM images of Fe_3O_4-SO_3H NPs (c) before use in reaction and (d) after five times applications.

A probable mechanism for the formation of products **4** and **5** has been depicted in Scheme 3 which emphasizes the role of nanomagnetite Fe_3O_4-SO_3H as an efficient acid catalyst. The mechanistic insight for the different mode of reactions of isatin and *N*-substituted isatins towards the formation of products **4** and **5** has been established unambiguously. During the formation of **4** and **5** the solid surface of Fe_3O_4-SO_3H nanoparticles transfers protons which catalyze the three component condensation reactions. Initially, the enaminone **3** condenses with the carbonyl group at position 3 of isatins (**1**) to generate the intermediate **6** which subsequently tautomerizes to intermediate **7**. When the starting material **1** is isatin (R_1 = H), the lone pair of nitrogen of enaminone moiety of intermediate **7** undergoes intramolecular nucleophilic attack to the amide carbonyl of isatin to

form a tetracyclic intermediate **10** which subsequently undergoes ring opening to generate intermediate **11**. Then the lone pair of free $–NH_2$ of intermediate **11** nucleophilically attacks the carbonyl carbon of indane-1,3-dione **2** to furnish the imine intermediate **12**. Finally, intramolecular cyclization of intermediate **13** followed by tautomerization of intermediate **14** leads to the formation of spiro compound **4**. But for *N*-substituted isatins (R_1=Alkyl/Aryl), the electrophilicity of amide carbonyl of isatins is diminished considerably; hence nucleophilic attack is not possible. Here, the enolic form of indane-1,3-dione (**2**) attacks the intermediate **7** to form the trione intermediate **8**. Subsequently intramolecular nuleophilic attack of the enamino nitrogen to the carbonyl carbon of indane-1,3-dione moiety of intermediate **8** leads to the formation of intermediate **9** which finally produces compound **5** through dehydration.

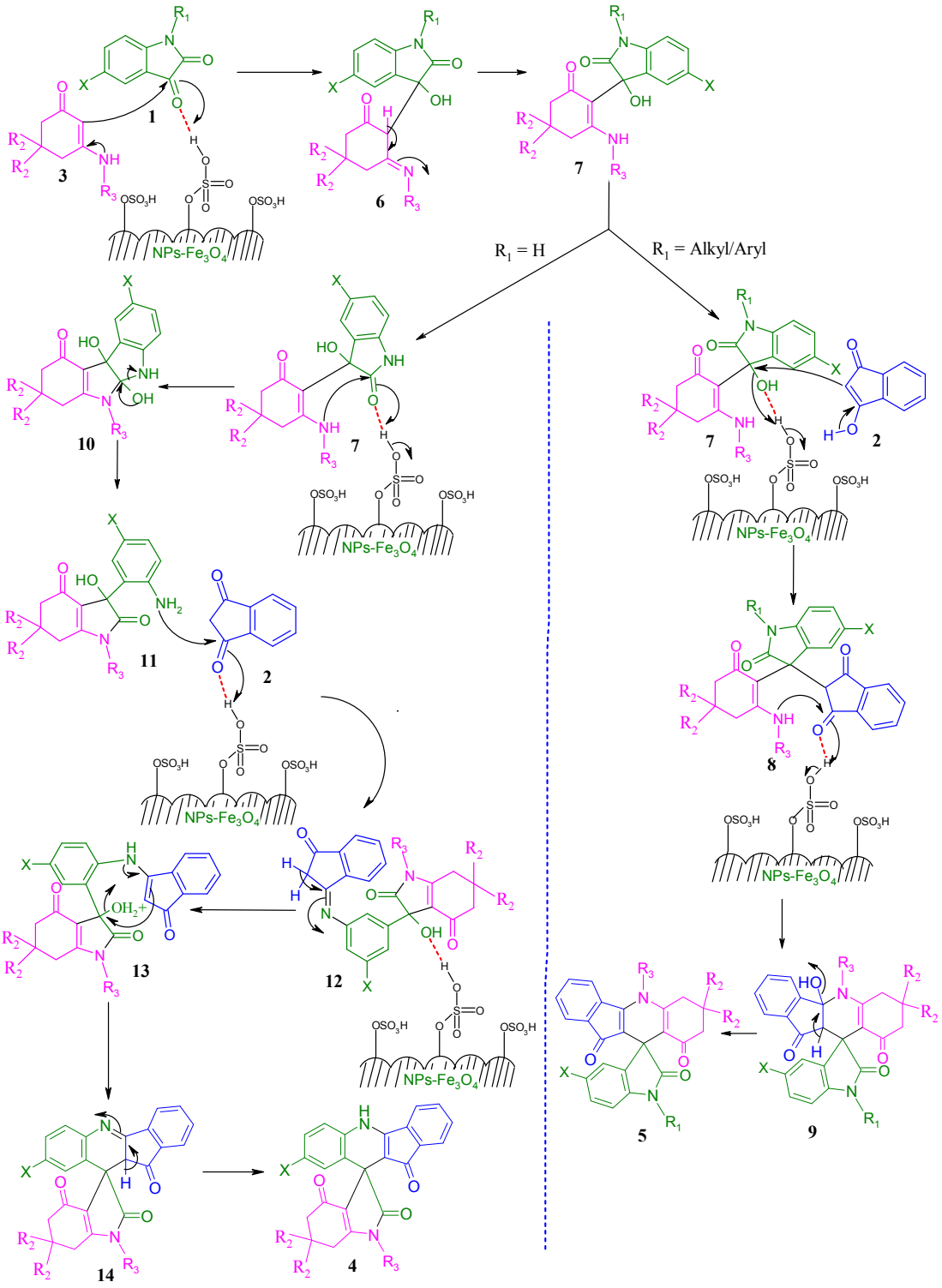

Scheme 3. Plausible mechanism for the formation of **4** and **5**.

The reusability test of Fe_3O_4-SO_3H nanoparticles was carried out separately for the synthesis of **4a** and **5a** under the optimized reaction conditions (Table 1, entry 18). After 2 h, at the end of the reactions, the reaction mixtures were ultrasonicated with ethyl acetate. As the products **4a** and **5a** were soluble in ethyl acetate, they were isolated from the surface of the solid support and the suspended magnetic Fe_3O_4-SO_3H nanoparticles were separated easily from the reaction mixture using an external magnetic bar without performing any filtration. Then Fe_3O_4-SO_3H nanoparticles were washed three times with ethyl acetate (3 x 5 mL), followed by washing with ethanol, dried at room temperature under vacuum to eliminate residual solvents and used for the next cycle. The multicomponent reactions for the synthesis of **4a** and **5a** were performed with the recovered catalyst upto five times. The result shows that there is indeed substantial retention of initial catalytic activity of Fe_3O_4-SO_3H nanoparticles even after repeated applications (Fig. 4).

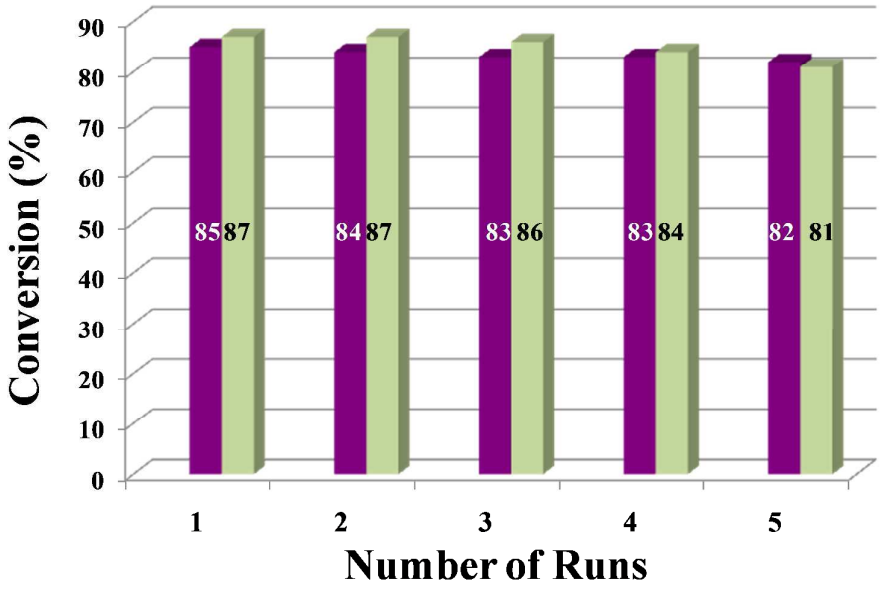

Figure 4. Reusability of Fe_3O_4-SO_3H MNPs for the formation of **4a** (purple bar) and **5a** (light green bar).

Conclusions

In summary, we have developed an efficient, green and sustainable methodology for the synthesis of two types of spiroindole fused dihydropyridine derivatives such as spiro[indolo-3,10′-indeno[1,2-*b*]quinolin]-2,4,11′-triones and indenoquinoline-spirooxindoles. The method involves one-pot condensation of isatins, indane-1,3-dione and enamines in presence of nano-magnetite Fe_3O_4-SO_3H as solid supported acid catalyst under solvent-free condition. In the reactions the surface of the solid Fe_3O_4-SO_3H transfers protons which catalyze the condensation to give the final products. The significant advantages of this methodology are the use of solvent-free reaction conditions, employment of simple and easily available starting materials and reagents, operational simplicity of the reaction and the use of a magnetically separable and recyclable catalyst. The reliable scalability and flexibility of structural modification as well as reaction generality are clearly represented in this transformation that provides an elegant and highly attractive methodology for the synthesis of such functionalized spirooxindole scaffolds of chemical and biomedical importance.

Experimental Section:

General methods:

Solvents and chemicals were purchased from commercial suppliers and used without further purification. Catalyst and starting materials were prepared according to reported procedure. Melting points were measured in open capillary tubes and were uncorrected. Perkin-Elmer 782 spectrophotometer was used for IR spectra. ^{1}H (300 MHz) and ^{13}C NMR (75 MHz) spectra were performed on Bruker instrument (300 MHz) in DMSO-d_6. Elemental analyses (C, H and N) were recorded using Perkin-Elmer 240C elemental analyzer. The X-ray diffraction data for crystallized compounds were collected with MoKα radiation at 296K using the Bruker APEX-II CCD System. The morphological analysis of the resultant nanoparticles was confirmed by TEM, monitored on a HRTEM, JEOL JEM 2010 at an

accelerating voltage of 200kV and fitted with a CCD camera. The crystallinity of synthesized $ZnFe_2O_4$ nanoparticles was determined and confirmed by XRD analysis. The diffractogram was documented from PANalytical, XPERT-PRO diffractrometer using Cu $_\alpha$ (λ= 1.54060) as X-ray source. Hitachi S-4800 Field Emission Scanning Electron Microscope (Hitachi S-4800 FE-SEM) operating voltage 5.0 kv is used for SEM.

General synthetic procedure for the preparation of compounds 4 and 5:

A mixture of isatins (1.0 mmol), indane-1,3-dione (1.0 mmol) and *N*-aryl/alkylenamines of 1,3-cyclohexadiones (1.0 mmol) was taken in a 100 ml round bottom flask and then minimum quantity of chloroform (5.0 ml) was added to the mixture for dissolving the substrates. The mixture was thoroughly mixed and soaked on the surface of nano Fe_3O_4-SO_3H solid support (500 mg) by stirring. Then the solvent was removed from the mixture under vacuum at 40 ºC. The resulting solid mixture was stirred at 85 ºC on an oil bath for 2h. Progress of the reaction was monitored by thin layer chromatography (TLC). At end of the reaction, ethyl acetate was added to the mixture and the product was extracted from the solid support by ultrasonication. The finely dispersed nano-particles were separated from the product solution by using an external magnetic bar and the separated organic phase was collected in another round bottom flask. The pure products **4** were obtained by evaporation of the solvent, followed by recrystallization from ethanol. Pure products **5** and few of the pure products **4** were obtained from isolated crude mass through column chromatography on silica gel using ethyl acetate/hexane (~1:1) as the eluent.

Characterization Data of 4a-n:

4a: Red amorphous solid, IR (KBr) 1714, 1675, 1612 cm^{-1}; ^1H NMR (300 MHz, DMSO-d_6) δ_H 10.88 (s, 1H), 7.64 (d, *J* = 7.2 Hz, 1H), 7.48 (t, *J* = 7.2 Hz, 1H), 7.39 (t, *J* = 7.2 Hz, 1H), 7.29-7.19 (m, 3H), 7.02-6.97 (m, 1H), 6.75 (d, *J* = 7.5 Hz, 1H), 3.63-3.56 (m, 2H), 2.82 (d, *J*

= 18.0 Hz, 1H), 2.67 (d, *J* = 17.7 Hz, 1H), 2.15 (d, *J* = 15.9 Hz, 1H), 2.04-1.99 (m, 1H), 1.63-1.56 (m, 2H), 1.43-1.36 (m, 2H), 1.11-1.06 (m, 6H), 0.95 (t, *J* = 7.5 Hz, 3H); ^{13}C NMR (75 MHz, DMSO-d_6) δ_H 189.8, 188.5, 181.2, 161.3, 156.3, 136.9, 136.4, 135.1, 131.6, 130.8, 128.7, 127.0, 124.7, 123.7, 121.1, 120.4, 119.4, 118.1, 101.1, 51.1, 49.1, 35.2, 34.4, 31.2, 29.1, 27.9, 19.8, 14.1; $C_{29}H_{28}N_2O_3$ (452.5): calcd. C 76.97, H 6.24, N 6.19; found C 76.80, H 6.05, N 6.08.

4b: Red amorphous solid, IR (KBr) 1746, 1607 cm^{-1}; ^{1}H NMR (300 MHz, DMSO-d_6) δ_H 11.01 (s, 1H), 7.81 (d, *J* = 8.4 Hz, 2H), 7.66 (d, *J* = 6.9 Hz, 1H), 7.46 (d, *J* = 8.1 Hz, 3H), 7.40 (t, *J* = 7.2 Hz, 1H), 7.31-7.22 (m, 3H), 7.06 (s, 2H), 2.69 (d, *J* = 18.0 Hz, 1H), 2.28-2.17 (m, 2H), 2.02 (d, *J* = 15.9 Hz, 1H), 1.04 (s, 3H), 1.00 (s, 3H); ^{13}C NMR (75 MHz, DMSO-d_6) δ_H 190.7, 188.9, 180.3, 159.6, 156.4, 137.0, 136.4, 135.1, 133.6, 133.0, 131.7, 131.0, 130.3, 129.0, 127.8, 125.0, 123.3, 122.2, 121.5, 120.5, 119.7, 118.3, 101.1, 51.3, 49.6, 36.2, 34.6, 29.3, 27.5; $C_{31}H_{23}BrN_2O_3$ (551.4): calcd. C 67.52, H 4.20, N 5.08; found C 67.70, H 4.25, N 4.98.

4c: Red amorphous solid, IR (KBr) 1746, 1674, 1632, 1608 cm^{-1}; ^{1}H NMR (300 MHz, DMSO-d_6) δ_H 10.92 (s, 1H), 7.58 (d, *J* = 8.1 Hz, 3H), 7.45 (d, *J* = 8.4 Hz, 2H), 7.39 (d, *J* = 7.2 Hz, 1H), 7.31 (t, *J* = 7.2 Hz, 1H), 7.20 (d, *J* = 6.3 Hz, 2H), 7.14 (d, *J* = 7.8 Hz, 1H), 6.97 (s, 2H), 2.60 (d, *J* = 18.0 Hz, 1H), 2.13-2.01 (m, 2H), 1.86 (d, *J* = 21.9 Hz, 1H), 0.95 (s, 3H), 0.90 (s, 3H); ^{13}C NMR (75 MHz, DMSO-d_6) δ_H 190.6, 188.9, 180.3, 159.6, 156.4, 137.0, 136.4, 135.1, 133.7, 133.1, 131.7, 131.0, 130.0, 129.8, 129.0, 127.8, 125.0, 123.3, 121.5, 120.5, 119.7, 118.2, 101.1, 51.3, 49.5, 36.2, 34.5, 29.3, 27.4; $C_{31}H_{23}ClN_2O_3$ (506.9): calcd. C 73.44, H 4.57, N 5.53; found C 73.30, H 4.45, N 5.39.

4d: Red amorphous solid, IR (KBr) 1700, 1650, 1608 cm^{-1}; ^{1}H NMR (300 MHz, DMSO-d_6) δ_H 10.96 (s, 1H), 7.67 (d, *J* = 6.9 Hz, 1H), 7.49-7.39 (m, 6H), 7.36-7.31 (m, 2H), 7.29-7.23

(m, 2H), 7.00 (t, *J* = 7.2 Hz, 1H), 6.83 (d, *J* = 7.5 Hz, 1H), 4.99 (d, *J* = 16.2 Hz, 1H), 4.83 (d, *J* = 7.5 Hz, 1H), 2.74 (d, *J* = 17.7 Hz, 1H), 2.43 (d, *J* = 18.0 Hz, 1H), 2.16 (d, *J* = 16.2 Hz, 1H), 2.01 (d, *J* = 15.9 Hz, 1H), 1.04 (s, 6H); ^{13}C NMR (75 MHz, DMSO-d_6) δ_H 190.1, 188.7, 181.2, 161.0, 156.5, 137.2, 136.8, 136.4, 135.1, 131.7, 130.9, 129.1, 128.9, 127.8, 127.1, 124.8, 123.6, 121.3, 120.5, 119.5, 118.3, 100.8, 51.1, 49.1, 43.7, 35.5, 34.4, 29.2, 27.8; $C_{32}H_{26}N_2O_3$ (486.5): calcd. C 78.99, H 5.39, N 5.76; found C 78.87, H 5.50, N 5.59.

4e: Red amorphous solid, IR (KBr) 1730, 1676, 1613 cm^{-1}; ^{1}H NMR (300 MHz, DMSO-d_6) δ_H 10.98 (s,1H), 7.66 (d, *J* = 6.9 Hz, 1H), 7.49 (t, *J* = 7.2 Hz, 1H), 7.42-7.37 (m, 5H), 7.30 (d, *J* = 7.2 Hz, 2H), 7.23 (d, *J* = 7.8 Hz, 1H), 6.90-6.89 (m, 2H), 2.64 (d, *J* = 17.7 Hz, 1H), 2.39 (s, 3H), 2.24-2.17 (m, 2H), 2.02 (d, *J* = 15.6 Hz, 1H), 1.03 (s, 3H), 1.01 (s, 3H); ^{13}C NMR (75 MHz, DMSO-d_6) δ_H 190.5, 188.8, 180.6, 160.3, 156.4, 138.8, 137.0, 136.4, 135.1, 131.6, 131.0, 130.4, 130.2, 128.9, 128.0, 127.6, 125.0, 123.5, 121.3, 120.5, 119.6, 118.2, 101.2, 51.3, 49.4, 36.3, 34.5, 29.3, 27.6, 21.2; $C_{32}H_{26}N_2O_3$ (486.5): calcd. C 78.99, H 5.39, N 5.76; found C 78.75, H 5.24, N 5.60.

4f: Red amorphous solid, IR (KBr) 1751, 1629, 1608 cm^{-1}; ^{1}H NMR (300 MHz, DMSO-d_6) δ_H 11.11 (s, 1H), 7.83 (d, *J* = 6.0 Hz, 1H), 7.65-7.23 (m, 9H), 7.06 (s, 1H), 2.73 (d, *J* = 18.0 Hz, 1H), 2.38 (s, 3H), 2.29-2.14 (m, 2H), 1.99 (d, *J* = 15.6 Hz, 1H), 1.04 (s, 3H), 0.99 (s, 3H); ^{13}C NMR (75 MHz, DMSO-d_6) δ_H 190.6, 188.8, 180.1, 161.0, 156.2, 138.9, 136.2, 134.8, 131.9, 131.5, 131.1, 130.4, 129.1, 128.6, 128.0, 127.2, 125.3, 120.8, 120.7, 119.8, 119.7, 101.0, 51.2, 49.5, 36.3, 34.5, 29.5, 27.3, 21.2; $C_{32}H_{25}ClN_2O_3$ (521.0): calcd. C 73.77, H 4.84, N 5.38; found C 73.61, H 4.67, N 5.20.

4g: Red amorphous solid, IR (KBr) 1748, 1679, 1635, 1610 cm^{-1}; ^{1}H NMR (300 MHz, DMSO-d_6) δ_H 10.99 (s, 1H), 7.66-7.57 (m, 3H), 7.51-7.37 (m, 4H), 7.31-7.21 (m, 3H), 7.10-7.01(m, 2H), 2.67-2.61 (m, 1H), 2.43-2.37 (m, 1H), 2.18 (t, *J* = 6.3 Hz, 2H), 2.01-1.92 (m,

2H); ^{13}C NMR (75 MHz, DMSO-d_6) δ_H 191.0, 188.8, 180.1, 161.4, 156.4, 137.0, 136.3, 135.1, 131.7, 131.0, 130.5, 130.4, 128.9, 127.9, 125.0, 123.4, 122.5, 120.5, 119.7, 118.1, 117.0, 116.7, 101.2, 49.6, 37.2, 22.7, 22.0; $C_{29}H_{19}FN_2O_3$ (462.47): calcd. C 75.32, H 4.14, N 6.06; found C 75.48, H 3.95, N 5.90.

4h: Red amorphous solid, IR (KBr) 1742, 1675, 1602 cm^{-1}; ^{1}H NMR (300 MHz, DMSO-d_6) δ_H 10.99 (s, 1H), 7.60 (d, *J* = 7.2 Hz, 1H), 7.47 (t, *J* = 7.5 Hz, 1H), 7.37 (d, *J* = 7.2 Hz, 1H), 7.33-7.19 (m, 3H), 6.74 (s, 1H), 3.68-3.52 (m, 2H), 2.86 (d, *J* = 17.7 Hz, 1H), 2.64 (d, *J* = 18.0 Hz, 1H), 2.21 (d, *J* = 15.9 Hz, 1H), 2.01 (d, *J* = 16.2 Hz, 1H), 1.62-1.55 (m, 2H), 1.42-1.33 (m, 2H), 1.10 (s, 3H), 1.09 (s, 3H), 0.93 (t, *J* = 7.2 Hz, 3H); ^{13}C NMR (75 MHz, DMSO-d_6) δ_H 190.0, 188.6, 180.8, 162.0, 156.2, 136.3, 136.1, 134.8, 131.8, 130.9, 128.9, 128.3, 126.7, 125.6, 120.8, 120.6, 119.7, 119.5, 100.9, 51.0, 49.1, 40.4, 35.2, 34.5, 31.2, 29.2, 27.8, 19.9, 14.1; $C_{29}H_{27}ClN_2O_3$ (487.0): calcd. C 71.52, H 5.59, N 5.75; found C 71.75, H 5.40, N 5.60.

4i: Red amorphous solid, IR (KBr) 1740, 1625, 1600 cm^{-1}; ^{1}H NMR (300 MHz, DMSO-d_6) δ_H 11.13 (s, 1H), 7.68-7.59 (m, 5H), 7.48 (d, *J* = 7.2 Hz, 2H), 7.41 (d, *J* = 6.6 Hz, 1H), 7.32 (s, 1H), 7.21-7.19 (m, 2H), 2.77 (d, *J* = 18 Hz, 1H), 2.29-2.18 (m, 2H), 2.01 (d, *J* = 16.2 Hz, 1H), 1.05 (s, 3H), 0.98 (s, 3H); ^{13}C NMR (75 MHz, DMSO-d_6) δ_H 190.8, 188.8, 179.9, 160.3, 156.2, 137.6, 136.6, 136.1, 134.8, 133.8, 133.0, 132.1, 131.9, 131.1, 130.2, 130.0, 125.4, 121.1, 120.8, 120.2, 119.8, 116.6, 101.0, 51.2, 49.5, 36.2, 34.6, 29.5, 27.3; $C_{31}H_{22}BrClN_2O_3$ (585.87): calcd. C 63.55, H 3.78, N 4.78; found C 63.35, H 3.67, N 4.70;

4j: Red amorphous solid, IR (KBr) 1748, 1634, 1610 cm^{-1}; ^{1}H NMR (300 MHz, DMSO-d_6) δ_H 11.16 (s, 1H), 7.90 (d, *J* = 5.7 Hz, 1H), 7.68-7.62 (m, 3H), 7.49 (d, *J* = 7.2 Hz, 2H), 7.41 (t, *J* = 7.5 Hz, 1H), 7.32-7.28 (m, 2H), 7.19 (d, *J* = 8.1 Hz, 1H), 2.75 (d, *J* = 17.7 Hz, 1H), 2.24 (d, *J* = 17.1 Hz, 2H), 2.01 (d, *J* = 15.6 Hz, 1H), 1.06 (s, 3H), 0.97 (s, 3H); ^{13}C NMR (75

MHz, DMSO-d_6) δ_H 190.8, 188.9, 179.9, 167.7, 160.0, 156.2, 156.0, 136.6, 136.1, 134.8, 132.1, 131.9, 131.2, 130.5, 130.4, 129.4, 125.3, 121.1, 120.8, 120.1, 119.8, 118.4, 118.1, 116.7, 101.0, 51.3, 49.5, 36.0, 34.5, 29.4, 27.3; $C_{31}H_{21}BrClFN_2O_3$ (603.8): calcd. C 61.66, H 3.51, N 4.64; found C 61.48, H 3.60, N 4.47.

4k: Red amorphous solid, IR (KBr) 1727, 1683, 1623 cm^{-1}; ^1H NMR (300 MHz, DMSO-d_6) δ_H 11.04 (s, 1H), 7.63 (d, J = 6.9 Hz, 1H), 7.49 (t, J = 7.8 Hz, 1H), 7.43-7.39 (m, 5H), 7.31 (d, J = 7.2 Hz, 1H), 7.26-7.24 (m, 1H), 7.20-7.14 (m, 1H), 6.95-6.92 (m, 1H), 2.70 (d, J = 17.7 Hz, 1H), 2.50 (s, 3H), 2.28-2.13 (m, 2H), 2.00 (d, J = 16.2 Hz, 1H), 1.05 (s, 3H), 1.00 (s, 3H); ^{13}C NMR (75 MHz, DMSO-d_6) δ_H 190.6, 188.8, 180.1, 161.0, 156.3, 138.8, 136.3, 135.0, 133.7, 133.8, 131.6, 131.0, 130.4, 128.0, 125.3, 125.3, 120.7, 120.6, 119.8, 119.6, 116.3, 116.0, 114.3, 114.0, 100.3, 51.3, 49.7, 36.3, 34.4, 29.6, 27.3, 21.2, 19.0; $C_{32}H_{25}FN_2O_3$: calcd. C 76.18, H 4.99, N 5.55; found C 76.00, H 4.85, N 5.49; HRMS: Calcd. *m/z*: 504.1849; Found: 505.2862 (M+1).

4l: Red amorphous solid, IR (KBr) 1747, 1631, 1612 cm^{-1}; ^1H NMR (300 MHz, DMSO-d_6) δ_H 11.14 (s, 1H), 7.94-7.92 (m, 2H), 7.70-7.61 (m, 3H), 7.50 (t, J = 7.5 Hz, 1H), 7.42 (d, J = 7.2 Hz, 1H), 7.38-7.28 (m, 2H), 7.24-7.22 (m, 1H), 2.67-2.50 (m, 1H), 2.44-2.43 (m, 1H), 2.21-2.18 (m, 2H), 2.04-1.96 (m, 2H); ^{13}C NMR (75 MHz, DMSO-d_6) δ_H 191.1, 188.8, 179.6, 161.6, 156.3, 137.7, 136.2, 136.1, 134.8, 131.9, 131.1, 130.6, 129.6, 129.5, 129.4, 129.1, 128.7, 127.8, 125.1, 122.1, 120.7, 120.4, 119.8, 119.7, 118.3, 118.0, 100.9, 49.7, 37.2, 22.7, 21.9; $C_{29}H_{17}Cl_2FN_2O_3$ (531.3): calcd. C 65.55, H 3.22, N 5.27; found C 65.37, H 3.05, N 5.12.

4m: Red amorphous solid, IR (KBr) 1716, 1678, 1616 cm^{-1}; ^1H NMR (300 MHz, DMSO-d_6) δ_H 10.94 (s, 1H), 7.60 (d, J = 7.2 Hz, 1H), 7.49-7.44 (m, 1H), 7.37 (t, J = 7.2 Hz, 1H), 7.27-7.20 (m, 2H), 7.16-7.12 (m, 1H), 6.62-6.58 (q, J_1 = 9.6 Hz, J_2 = 2.7 Hz 1H), 3.63-3.53 (m,

2H), 2.85 (d, *J* = 17.7 Hz, 1H), 2.64 (d, *J* = 17.7 Hz, 2H), 2.21 (d, *J* = 15.9 Hz, 1H), 2.01 (d, *J* = 15.9 Hz, 1H), 1.59 (t, *J* = 7.2 Hz, 2H), 1.41-1.34 (m, 2H), 1.10 (s, 6H), 0.93 (t, *J* = 7.2 Hz, 3H); ^{13}C NMR (75 MHz, DMSO-d_6) δ_H 190.0, 188.6, 180.8, 161.9, 160.9, 157.7, 156.3, 136.3, 135.0, 133.6, 131.6, 130.9, 125.6, 125.5, 120.6, 120.5, 119.7, 119.6, 119.4, 116.1, 115.8, 113.6, 113.3, 100.1, 51.1, 49.3, 35.3, 34.4, 31.2, 29.4, 27.7, 19.8, 14.1; $C_{29}H_{27}FN_2O_3$: calcd. C 74.02, H 5.78, N 5.95; found C 73.89, H 5.55, N 5.77; HRMS: Calcd. *m/z*: 470.2006; Found: 471.4313 (M+1).

4n: Red amorphous solid, IR (KBr) 1702, 1652, 1607 cm^{-1}; ^{1}H NMR (300 MHz, DMSO-d_6) δ_H 11.07 (s, 1H), 7.64 (d, *J* = 6.9 Hz, 1H), 7.50 (d, *J* = 6.9 Hz, 3H), 7.45-7.36 (m, 3H), 7.31 (d, *J* = 7.2 Hz, 3H), 7.24 (d, *J* = 8.7 Hz, 1H), 6.87 (s, 1H), 5.02 (d, *J* = 16.5 Hz, 1H), 4.83 (1H, *J* = 16.5 Hz, 1H), 2.84-2.78 (m, 1H), 2.52-2.39 (m, 1H), 2.17-2.09 (m, 2H), 1.99 (d, *J* = 5.7 Hz, 2H); ^{13}C NMR(75MHz, DMSO-d_6) δ_H 190.4, 188.4, 180.4, 162.8, 156.3, 136.9, 136.0, 135.8, 134.6, 131.6, 130.8, 128.9, 128.8, 128.3, 127.7, 127.2, 126.6, 125.4, 121.8, 120.5, 119.5, 119.4 , 100.4, 49.0, 43.8, 36.7, 22.1, 21.7; $C_{30}H_{21}ClN_2O_3$ (492.95): calcd. C 73.09, H 4.29, N 5.68; found C 72.89, H 4.14, N 5.57.

Characterization Data of 5a-s

5a: Red amorphous solid, IR (KBr) 1705, 1689, 1657 cm^{-1}; ^{1}H NMR (300 MHz, DMSO-d_6) δ_H 7.45 (d, *J* = 7.5 Hz, 1H), 7.35 (t, *J* = 7.5 Hz, 1H), 7.23 (t, *J* = 7.2 Hz, 1H), 7.11-7.01 (m, 2H), 7.01-6.79 (m, 2H), 6.72 (t, *J* = 7.2 Hz, 1H), 4.05-4.01 (m, 2H), 3.65-3.57 (m, 2H), 2.62-2.70 (m, 2H), 2.04 (d, *J* = 15.9 Hz, 1H), 1.89 (d, *J* = 15.9 Hz, 1H), 1.66 (t, *J* = 7.5 Hz, 2H), 1.42-1.35 (m, 2H), 1.15 (t, *J* = 6.9 Hz, 3H), 0.96 (s, 3H), 0.90-0.85 (m, 6H); ^{13}C NMR (75 MHz, DMSO-d_6) δ_H 194.6, 189.5, 177.2, 156.0, 153.8, 143.3, 136.4, 135.3, 133.1, 133.0, 130.5, 128.1, 122.8, 122.7, 121.6, 121.3, 115.3, 111.1, 107.6, 49.7, 47.0, 46.4, 39.1, 34.5, 33.1, 32.3, 28.4, 27.2, 19.3, 14.0, 12.1. $C_{31}H_{32}N_2O_3$: calcd. C 77.47, H 6.71, N 5.83; found C 77.28, H 6.60, N 5.66; HRMS: Calcd. *m/z*: 480.2413; Found: 481.3737 (M+1).

5b: Red amorphous solid, IR (KBr) 1721, 1695, 1675 cm^{-1}; ^{1}H NMR (300 MHz, DMSO-d_6) δ_H 7.72-7.69 (m, 1H), 7.63-7.60 (m, 1H), 7.25 (d, *J* = 7.5 Hz, 1H), 7.20-7.14 (m, 5H), 7.08-7.02 (m, 1H), 6.93 (d, *J* = 7.5 Hz, 1H), 6.87 (t, *J* = 7.5 Hz, 1H), 5.31 (d, *J* = 7.5 Hz, 1H), 3.89 (s, 3H), 3.64 (t, *J* = 7.2 Hz, 2H), 2.48-2.45 (m, 1H), 2.39-2.12 (m, 3H), 1.84-1.71 (m, 4H), 1.01 (t, *J* = 7.5 Hz, 3H); ^{13}C NMR (75 MHz, DMSO-d_6) δ_H 195.0, 189.8, 177.7, 160.6, 155.4, 154.8, 144.0, 136.7, 135.5, 132.9, 132.4, 130.8, 130.4, 128.2, 123.7, 121.7, 121.5, 121.2, 115.6, 115.5, 115.3, 110.0, 107.7, 56.1, 47.2, 41.9, 36.7, 27.6, 21.0, 20.7, 11.9; $C_{33}H_{28}N_2O_4$: calcd. C 76.73, H 5.46, N 5.42; found C 76.58, H 5.30, N 5.31; HRMS: Calcd. *m/z*: 516.2049; Found: 517.2151 (M+1).

5c: Red amorphous solid, IR (KBr) 1727, 1673, 1635, 1612 cm^{-1}; ^{1}H NMR (300 MHz, DMSO-d_6) δ_H 7.59 (d, *J* = 7.5 Hz, 1H), 7.46-7.37 (m, 4H), 7.34-7.33 (m, 3H), 7.31-7.26 (m, 3H), 7.01 (t, *J* = 7.5 Hz, 1H), 6.80 (d, *J* = 7.8 Hz, 1H), 4.92 (d, *J* = 16.2 Hz, 1H), 4.77 (d, *J* = 16.2 Hz, 1H), 4.28 (t, *J* = 7.2 Hz, 2H), 2.73-2.67 (m, 1H), 2.46-2.42 (m, 1H), 2.08-2.06 (m, 2H), 1.91-1.85 (m, 4H), 1.05 (t, *J* = 7.2 Hz, 3H); ^{13}C NMR (75 MHz, DMSO-d_6) δ_H 190.4, 188.3, 180.9, 162.1, 158.3, 138.7, 137.2, 136.6, 135.3, 132.3, 130.7, 129.1, 127.9, 127.4, 127.1, 125.2, 125.0, 122.9, 122.6, 120.9, 116.6, 103.5, 49.2, 48.1, 43.8, 36.9, 22.5, 22.3, 21.8, 10.8. $C_{33}H_{28}N_2O_3$ (500.5): calcd. C 79.18, H 5.64, N 5.60; found C 78.97, H 5.55, N 5.49.

5d: Red amorphous solid, IR (KBr) 1725, 1680, 1630 cm^{-1}; ^{1}H NMR (300 MHz, DMSO-d_6) δ_H 7.88 (d, *J* = 8.4 Hz, 2H), 7.82 (d, *J* = 7.8 Hz, 1H), 7.71 (d, *J* = 7.8 Hz, 1H), 7.28 (d, *J* = 7.2 Hz, 1H), 7.22-7.14 (m, 3H), 7.08 (t, *J* = 7.2 Hz, 1H), 6.94 (d, *J* = 7.8 Hz, 1H), 6.87 (t, *J* = 7.2 Hz, 1H), 5.30 (d, *J* = 7.5 Hz, 1H), 3.70-3.62 (m, 2H), 2.44-2.38 (m, 1H), 2.24-2.14 (m, 3H), 1.83-1.73 (m, 4H), 1.01 (t, *J* = 7.8 Hz, 3H); ^{13}C NMR(75MHz, DMSO-d_6) δ_H 195.0, 189.8, 177.6, 154.8, 154.1, 144.0, 137.7, 136.5, 135.4, 133.6, 133.4, 132.8, 132.6, 130.5, 128.4, 124.2, 123.8, 121.8, 121.5, 121.3, 115.7, 110.4, 107.8, 47.2, 42.0, 36.8, 27.7, 21.0, 20.7, 12.0; $C_{32}H_{25}BrN_2O_3$ (565.45): calcd. C 67.97, H 4.46, N 4.95; found C 67.78, H 4.30, N 4.78.

5e: Red amorphous solid, IR (KBr) 1727, 1684, 1623 cm^{-1}; ^1H NMR (300 MHz, DMSO-d_6) δ_H 8.06 (d, *J* = 8.7 Hz, 1H), 7.80-7.77 (m, 3H), 7.46 (d, *J* = 2.1 Hz, 1H), 7.28-7.19 (m, 3H), 7.15-7.10 (m, 1H), 7.02 (d, *J* = 8.4 Hz, 1H), 5.29 (d, *J* = 7.5 Hz, 1H), 3.81-3.75 (m, 2H), 2.38 (d, *J* = 17.4 Hz, 1H), 2.23-1.99 (m, 3H), 1.26 (t, *J* = 7.2 Hz, 3H), 0.95 (s, 3H), 0.89 (s, 3H); ^{13}C NMR(75MHz, DMSO-d_6) δ_H 195.1, 189.8, 176.9, 154.8, 153.2, 152.3, 149.8, 142.5, 137.1, 136.5, 135.7, 132.7, 132.6, 130.7, 130.5, 128.2, 126.1, 124.1, 121.6, 121.5, 114.1, 109.2, 49.9, 47.5, 41.3, 34.8, 32.5, 28.7, 27.0, 12.1. $C_{33}H_{26}Cl_2N_2O_3$ (569.47): calcd. C 69.60, H 4.60, N 4.92; found C 69.18, H 4.43, N 4.95.

5f: Red amorphous solid, IR (KBr) 1728, 1685, 1639 cm^{-1}; ^1H NMR (300 MHz, DMSO-d_6) δ_H 8.00-7.99 (m, 1H), 7.71-7.69 (m, 1H), 7.48-7.46 (m, 2H), 7.36 (s, 1H), 7.15-7.12 (m, 3H), 7.05-7.00 (m, 1H), 6.93 (d, *J* = 8.4 Hz, 1H), 5.15 (d, *J* = 7.5 Hz, 1H), 3.61-3.54 (m, 2H), 2.29 (d, *J* = 17.4 Hz, 1H), 2.12-1.90 (m, 3H), 1.67-1.60 (m, 2H), 0.93 (t, *J* = 7.2 Hz, 3H), 0.87 (s, 3H), 0.80 (s, 3H); ^{13}C NMR(75MHz, DMSO-d_6) δ_H 194.9, 189.6, 177.2, 164.5, 161.2, 154.8, 153.3, 143.0, 136.9, 136.4, 134.4, 132.9, 132.6, 132.4, 130.4, 127.9, 125.8, 123.7, 121.4, 117.5, 117.4, 117.0, 113.9, 109.0, 49.7, 47.2, 41.8, 32.2, 28.4, 26.9, 20.5, 11.7; $C_{34}H_{28}ClFN_2O_3$: calcd. C 72.02, H 4.98, N 4.94; found C 72.23, H 5.10, N 4.90; HRMS: Calcd. *m/z*: 566.1772; Found: 567.3985 (M+1).

5g: Red amorphous solid, IR (KBr) 1720, 1671, 1632, 1611 cm^{-1}; ^1H NMR (300 MHz, DMSO-d_6) δ_H 7.44 (t, *J* = 7.5 Hz, 2H), 7.34 (t, *J* = 7.2 Hz, 2H), 7.30 (d, *J* = 7.2 Hz, 1H), 7.24-7.22 (m, 2H), 7.18-7.15 (m, 2H), 7.12 (d, *J* = 8.4 Hz, 1H), 6.95 (d, *J* = 8.4 Hz, 1H), 5.45 (s, 1H), 3.64-3.58 (q, J_1 = 6.9 Hz, J_2 = 3.6 Hz, 2H), 2.80-2.74 (m, 1H), 2.59-2.53 (m, 1H), 2.14-2.10 (m, 2H), 1.87-1.79 (m, 2H), 1.71-1.64 (m, 2H), 1.25-1.10 (m, 2H), 0.85 (t, *J* = 8.1 Hz, 3H); ^{13}C NMR(75MHz, DMSO-d_6) δ_H 194.9, 189.7, 177.4, 157.1, 156.9, 143.2, 137.5, 137.3, 136.1, 133.0, 130.7, 129.7, 128.1 128.0, 125.9, 125.8, 123.4, 122.9, 121.6,

116.3, 110.5, 109.2, 50.8, 47.5, 42.0, 36.4, 29.4, 26.1, 21.3, 20.7, 11.9; $C_{33}H_{27}ClN_2O_3$ (535.03): calcd. C 74.08, H 5.09, N 5.24; found C 73.88, H 4.95, N 5.06.

5h: Red amorphous solid, IR (KBr) 1728, 1695, 1670 cm^{-1}; ^1H NMR (300 MHz, DMSO-d_6) δ_H 7.66 (d, *J* = 7.2 HZ, 1H), 7.54 (d, *J* = 7.2 Hz, 1H), 7.45 (d, *J* = 8.1 Hz, 2H), 7.25 (d, *J* = 7.2 Hz, 1H), 7.18-7.10 (m, 3H), 7.02-6.98 (m, 1H), 6.87 (t, *J* = 7.2Hz, 1H), 6.79 (d, *J* = 7.5 Hz, 1H), 5.99-5.90 (m, 1H), 5.65 (d, *J* = 17.4 Hz, 1H), 5.19 (d, *J* = 7.5 Hz, 2H), 4.38-4.32 (m, 2H), 2.45 (s, 3H), 2.36 (d, *J* = 10.8Hz, 1H), 2.17 (d, *J* = 15.9 Hz, 1H), 1.99-1.91 (m, 2H), 0.89 (s, 3H), 0.81 (s, 3H); ^{13}C NMR(75MHz, DMSO-d_6) δ_H 194.9, 189.8, 177.5, 154.8, 153.1, 143.4, 140.6, 136.6, 135.6, 135.0, 132.8, 132.3, 131.1, 130.8, 130.4, 129.8, 128.2, 123.4, 122.0, 121.4, 121.3, 117.1, 114.3, 109.8, 108.4, 49.9, 47.1, 42.6, 40.7, 32.3, 28.9, 26.6, 21.3; $C_{35}H_{30}N_2O_3$ (526.62): calcd. C 79.82, H 5.74, N 5.32; found C 79.61, H 5.40, N 5.15.

5i: Red amorphous solid, IR (KBr) 1724, 1690, 1665, 1615 cm^{-1}; ^1H NMR (300 MHz, DMSO-d_6) δ_H 7.52 (d, *J* = 6.9 Hz, 3H), 7.45-7.40 (m, 3H), 7.37-7.32 (m, 3H), 7.28 (d, *J* = 6.3 Hz, 2H), 7.07-7.02 (m, 1H), 6.86 (d, *J* = 7.8 Hz, 1H), 6.28-6.19 (m, 1H), 5.40-5.32 (m, 2H), 5.01 (s, 2H), 4.97 (s, 1H), 4.84 (d, *J* = 16.2 Hz, 1H), 2.78-2.72 (m, 1H), 2.47-2.45 (m, 1H), 2.13-2.12 (m, 2H), 1.96-1.94 (m, 2H); ^{13}C NMR(75MHz, DMSO-d_6) δ_H 190.5, 188.5, 181.0, 162.1, 158.7, 139.0, 137.2, 136.2, 135.1, 133.6, 132.2, 130.6, 129.1, 128.9, 127.9, 127.5, 127.4, 127.3, 127.3, 126.9, 125.2, 124.8, 123.1, 122.8, 120.9, 116.8, 116.7, 103.6, 49.7, 49.1, 43.9, 40.8, 36.9, 22.2, 21.9; $C_{33}H_{26}N_2O_3$ (498.57): calcd. C 79.50, H 5.26, N 5.62; found C 79.28, H 5.30, N 5.66.

5j: Red amorphous solid, IR (KBr) 1726, 1699, 1668 cm^{-1}; ^1H NMR (300 MHz, DMSO-d_6) δ_H 8.53-8.51 (q, J_1 = 6.6 Hz, J_2 = 2.1 Hz, 1H), 7.88-7.86 (m, 1H), 7.81-7.76 (m, 1H), 7.59-7.50 (m, 1H), 7.25-7.17 (m, 4H), 6.86 (d, *J* = 8.4 Hz, 1H), 5.96-5.91 (m, 1H), 5.67 (d, *J* =

17.4 Hz, 1H), 5.36-5.32 (m, 1H), 5.24 (d, *J* = 10.3 Hz, 1H), 4.42-4.28 (m, 2H), 2.41 (d, *J* = 17.7 Hz, 1H), 2.22-1.99 (m, 3H), 0.97 (s, 3H), 0.90 (s, 3H); ^{13}C NMR (75MHz, DMSO-d_6) δ_H 195.2, 189.9, 177.3, 154.8, 153.3, 142.6, 136.8, 136.5, 135.1, 133.1, 132.9, 132.7, 132.5, 130.7, 128.1, 126.4, 124.1, 124.0, 121.7, 121.4, 118.7, 117.4, 114.1, 109.8, 109.4, 50.0, 47.4, 42.8, 32.5, 28.8, 28.6, 27.1, 26.9; $C_{34}H_{25}Cl_2FN_2O_3$ (599.47): calcd. C 68.12, H 4.20, N 4.67; found C 67.97, H 4.01, N 4.48.

5k: Red amorphous solid, IR (KBr) 1727, 1697, 1672 cm^{-1}; ^{1}H NMR (300 MHz, DMSO-d_6) δ_H 7.99 (d, *J* = 7.8 Hz, 1H), 7.91 (d, *J* = 7.8 Hz, 1H), 7.81 (t, *J* = 7.5 Hz, 1H), 7.74-7.72 (m, 1H), 7.22-7.19 (m, 2H), 7.15 (d, *J* = 7.8 Hz, 1H), 7.09-7.07 (m, 1H), 6.94 (t, *J* = 7.2 Hz, 1H), 6.87 (d, *J* = 7.5 Hz, 1H), 6.09-5.91 (m, 1H), 5.70 (d, *J* = 17.4 Hz, 1H), 5.26-5.15 (m, 2H), 4.43-4.30 (m, 2H), 0.95 (s, 3H), 2.28 (d, *J* = 15.9 Hz, 1H), 2.01 (d, *J* = 15.6 Hz, 2H), 1.82 (d, *J* = 17.4 Hz, 1H), 0.89 (s, 3H); ^{13}C NMR (75MHz, DMSO-d_6) δ_H 195.0, 189.9, 177.4, 154.3, 152.5, 143.6, 136.2, 135.2, 135.0, 134.5, 133.3, 132.9, 132.8, 132.7, 132.5, 131.2, 130.8, 129.6, 128.5, 123.1, 122.4, 121.8, 120.2, 117.3, 114.5, 110.4, 108.8, 49.9, 47.2, 42.8, 32.3, 31.1, 29.4, 26.1; $C_{34}H_{27}ClN_2O_3$ (547.04): calcd. C 74.65, H 4.97, N 5.12; found C 74.42, H 4.83, N 5.02.

5l: Red amorphous solid, IR (KBr) 1723, 1698, 1671 cm^{-1}; ^{1}H NMR (300 MHz, DMSO-d_6) δ_H 8.34 (s, 1H), 8.04-8.00 (m, 1H), 7.84 (d, *J* = 7.5 Hz, 1H), 7.76-7.71 (m, 1H), 7.60 (s, 1H), 7.25-7.23 (m, 3H), 7.13-7.07 (m, 1H), 6.86 (d, *J* = 8.1 Hz, 1H), 6.00-5.91 (m, 1H), 5.68 (d, *J* = 17.1 Hz, 1H), 5.25-5.19 (m, 2H), 4.43-4.30 (m, 2H), 2.41 (d, *J* = 18.6 Hz, 1H), 2.23-2.03 (m, 3H), 0.97 (s, 3H), 0.91 (s, 3H); ^{13}C NMR (75MHz, DMSO-d_6) δ_H 189.4, 184.1, 171.5, 148.9, 147.3, 136.8, 133.7, 131.1, 130.7, 129.1, 126.8, 126.7, 126.1, 125.5, 124.9, 123.6, 122.3, 120.6, 118.3, 115.9, 115.6, 111.6, 108.2, 104.0, 44.1, 41.7, 37.0, 26.7, 22.7, 21.4;

$C_{34}H_{26}Cl_2N_2O_3$: calcd. C 70.23, H 4.51, N 4.82; found C 70.05, H 4.98, N 4.57; HRMS: Calcd. *m/z*: 580.1320; Found: 581.1368 (M+1).

5m: Red amorphous solid, IR (KBr) 1718, 1692, 1652 cm^{-1}; ^1H NMR (300 MHz, DMSO-d_6) δ_H 10.26 (s, 1H), 7.49 (t, *J* = 7.5 Hz, 1H), 7.27-7.15 (m, 5H), 7.11-7.06 (m, 2H), 7.00 (d, *J* = 6.0 Hz, 1H), 6.96 (s, 1H), 6.91 (t, *J* = 6.9 Hz, 1H), 5.40-5.36 (q, J_1 = 7.2 Hz, J_2 = 2.7 Hz, 1H), 3.79-3.76 (m, 2H), 2.19-2.15 (m, 1H), 2.21-2.15 (m, 2H), 1.96 (d, *J* = 12.0 Hz, 1H), 1.29 (t, *J* = 7.2 Hz, 3H), 0.95 (s, 3H), 0.86 (s, 3H); ^{13}C NMR (75MHz, DMSO-d_6) δ_H 194.5, 189.4, 176.8, 158.8, 158.5, 154.2, 152.5, 143.0, 138.7, 136.2, 134.9, 132.5, 132.1, 130.1, 128.0, 123.2, 121.5, 121.1, 120.9, 120.2, 117.6, 116.5, 113.9, 109.6, 107.4, 49.6, 46.8, 34.3, 32.0, 28.7, 28.6, 26.2, 11.9; $C_{33}H_{28}N_2O_4$ (516.58): calcd. C 76.73, H 5.46, N 5.42; found C 76.54, H 5.30, N 5.29.

5n: Red amorphous solid, IR (KBr) 1707, 1695, 1646 cm^{-1}; ^1H NMR (300 MHz, DMSO-d_6) δ_H 8.04-7.93 (m, 3H), 7.82-7.75 (m, 1H), 7.69 (d, *J* = 7.8 Hz, 2H), 7.62-7.60 (m, 2H), 7.54 (d, *J* = 7.2 Hz, 1H), 7.48 (d, *J* = 7.2 Hz, 1H), 7.30 (d, *J* = 4.2 Hz, 2H), 7.23-7.15 (m, 2H), 7.04 (t, *J* = 7.2 Hz, 1H), 6.71 (d, *J* = 7.8 Hz, 1H), 5.38 (d, *J* = 7.5 Hz, 1H), 2.55-2.51 (m, 1H), 2.33 (d, *J* = 15.9 Hz, 1H), 2.15-2.07 (m, 2H), 1.02 (s, 3H), 0.95 (s, 3H); ^{13}C NMR (75MHz, DMSO-d_6) δ_H 195.3, 190.1, 177.2, 154.5, 153.0, 143.9, 137.5, 136.6, 135.9, 134.6, 133.8, 132.7, 132.6, 131.3, 130.7, 130.0, 129.9, 128.6, 128.1, 127.3, 127.2, 124.3, 122.7, 121.7, 121.5, 114.6, 110.4, 108.2, 49.9, 47.3, 40.7, 32.5, 29.6, 26.6; $C_{37}H_{27}BrN_2O_3$ (627.52): calcd. C 70.82, H 4.34, N 4.46; found C 70.65, H 4.15, N 4.25.

5o: Red amorphous solid, IR (KBr) 1710, 1699, 1645 cm^{-1}; ^1H NMR (300 MHz, DMSO-d_6 8.03-7.92 (m, 2H), 7.79-7.77 (m, 1H), 7.63-7.59 (m, 4H), 7.50-7.47 (m, 2H), 7.33-7.26 (m, 2H), 7.17 (d, *J* = 6.6 Hz, 2H), 7.00 (d, *J* = 6.9 Hz, 1H), 6.66 (d, *J* = 5.4 Hz, 1H), 5.38 (s, 1H), 2.51-2.47 (m, 1H), 2.30-1.99 (m, 3H), 0.91 (s, 3H), 0.87 (s, 3H); ^{13}C NMR (75MHz, DMSO-

d_6) δ_H 189.4, 184.3, 171.4, 148.7, 147.2, 138.1, 130.8, 130.2, 129.3, 128.8, 127.1, 126.9, 125.8, 124.8, 124.3, 124.1, 122.7, 122.5, 122.3, 121.5, 121.1, 118.8, 117.4, 116.9, 115.9, 115.7, 112.9, 108.8, 104.1, 102.4, 44.2, 41.5, 28.8, 26.8, 25.6, 23.4, 23.2; $C_{37}H_{26}ClFN_2O_3$ (601.06): calcd. C 73.93, H 4.36, N 4.66; found C 73.63, H 4.25, N 4.40.

5p: Red amorphous solid, IR (KBr) 1705, 1693, 1650 cm^{-1}; ^1H NMR (300 MHz, DMSO-d_6) δ_H 10.26 (s, 1H), 7.65-7.55 (m, 4H), 7.49 (d, J = 7.5 Hz, 2H), 7.36 (t, J = 6.9 Hz, 1H), 7.28-7.23 (m, 3H), 7.19-7.08 (m, 4H), 7.04-6.96 (m, 1H), 6.66 (d, J = 7.8 Hz, 1H), 5.43-5.40 (q, J_1 = 7.2 Hz, J_2 = 3.0 Hz, 1H), 2.58-2.51 (m, 1H), 2.33-1.99 (m, 3H), 0.98 (s, 3H), 0.91 (s, 3H); ^{13}C NMR (75MHz, DMSO-d_6) δ_H 189.4, 184.3, 171.5, 153.5, 153.1, 148.9, 147.4, 138.1, 133.2, 130.8, 130.1, 128.9, 127.0, 126.8, 125.7, 125.4, 124.8, 124.1, 122.7, 122.3, 121.4, 118.2, 117.0, 115.9, 115.7, 114.9, 112.4, 112.2, 111.2, 108.6, 104.2, 102.5, 44.1, 41.5, 26.7, 23.4, 20.8; $C_{37}H_{28}N_2O_4$: calcd. C 78.71, H 5.00, N 4.96; found C 78.52, H 4.85, N 4.78; HRMS: Calcd. *m/z*: 564.2049; Found: 565.5298 (M+1).

5q: Red amorphous solid, IR (KBr) 1704, 1689, 1655 cm^{-1}; ^1H NMR (300 MHz, DMSO-d_6) δ_H 7.76-7.69 (m, 5H), 7.25-7.23 (2H, m), 7.17 (t, J = 8.1 Hz, 1H), 7.08-7.04 (m, 2H), 6.86 (d, J = 6.9 Hz, 1H), 6.54 (d, J = 7.2 Hz, 1H), 5.36 (d, J = 7.2 Hz, 1H), 3.70-3.64 (m, 2H), 2.90-2.78 (m, 2H), 2.19 (d, J = 5.4 Hz, 2H), 1.69-1.62 (m, 2H), 1.47-1.40 (m, 2H), 1.26-1.16 (m, 2H), 0.98 (t, J = 6.9 Hz, 3H); ^{13}C NMR (75MHz, DMSO-d_6) δ_H 190.1, 188.4, 180.5, 161.9, 156.6, 139.9, 138.4, 136.5, 134.3, 131.2, 130.4, 130.1, 128.2, 126.8, 124.9, 124.0, 122.4, 121.0, 120.3, 116.7, 103.1, 59.8, 48.7, 40.0, 36.6, 30.7, 21.6, 21.5, 19.6, 14.1; $C_{33}H_{28}N_2O_3$ (500.58): calcd. C 79.18, H 5.64, N 5.60; found C 78.93, H 5.40, N 5.48.

5r: Red amorphous solid, IR (KBr) 1726, 1698, 1653 cm^{-1}; ^1H NMR (300 MHz, DMSO-d_6) δ_H 7.76 (d, J = 7.2 Hz, 1H), 7.69-7.65 (m, 1H), 7.56 (d, J = 8.1 Hz, 3H), 7.48 (d, J = 8.1 Hz, 2H), 7.40 (d, J = 7.2 Hz, 1H), 7.27 (d, J = 7.2 Hz, 1H), 7.17-7.14 (m, 2H), 7.05-6.99 (m, 2H),

6.86-6.81 (1H, m), 6.54 (d, *J* = 7.8 Hz, 1H), 5.14-5.11 (m, 1H), 4.86 (s, 2H), 2.50-2.37 (1H, m), 2.17 (d, *J* = 16.2 Hz, 1H), 2.03-1.91 (m, 2H), 0.88 (s, 3H), 0.80 (s, 3H); ^{13}C NMR (75MHz, DMSO-d_6) δ_H 195.1, 189.9, 177.9, 154.5, 152.8, 143.2, 139.4, 136.7, 136.5,134.8, 134.5, 132.6, 132.2, 131.9, 131.6, 131.3, 130.6, 130.0, 129.4, 128.4, 124.2, 122.3, 121.6, 121.2, 120.6, 114.3, 110.1, 108.4, 50.0, 47.1, 43.6, 32.5, 28.9, 26.6; $C_{38}H_{28}BrClN_2O_3$ (675.99): calcd. C 67.52, H 4.17, N 4.14; found C 67.33, H 4.15, N 4.00.

5s: Red amorphous solid, IR (KBr) 1728, 1693, 1651 cm^{-1}; ^{1}H NMR (300 MHz, DMSO-d_6) δ_H 7.95 (d, *J* = 7.2 Hz, 1H), 7.78 (d, *J* = 7.8 Hz, 3H), 7.65 (d, *J* = 8.4 Hz, 2H), 7.55 (d, *J* = 8.4 Hz, 2H), 7.36 (d, *J* = 7.5 Hz, 1H), 7.25-7.21 (m, 2H), 7.13-7.07 (m, 2H), 6.91 (t, *J* = 7.5 Hz, 1H), 6.62 (d, *J* = 7.8 Hz, 1H), 5.30 (d, *J* = 7.5 Hz, 1H), 4.94 (s, 2H), 2.49-2.43 (m, 1H), 2.28-2.07 (m, 1H), 2.04-2.03 (m, 1H), 1.98 (s, 1H), 0.95 (s, 3H), 0.86 (s, 3H); ^{13}C NMR (75MHz, DMSO-d_6) δ_H 195.1, 189.9, 177.9, 154.6, 153.1, 143.2, 137.1, 136.7, 136.5, 135.6, 134.9, 132.7, 132.6, 132.3, 131.6, 130.8, 130.6, 130.5, 130.0, 128.4, 123.8, 122.3, 121.6, 121.4, 120.5, 114.4, 110.1, 108.5, 60.1, 49.9, 43.6, 40.8, 32.4, 29.0, 26.5; $C_{38}H_{28}Br_2N_2O_3$ (720.44): calcd. C 63.35, H 3.92, N 3.89; found C 63.10, H 3.78, N 3.78.

Acknowledgements

K.D. and K.S. thank UGC, New Delhi, India for offering them Senior Research Fellowship (SRF) and Junior Research Fellowship (JRF) respectively. The financial assistance of CSIR, New Delhi is gratefully acknowledged [Major Research Project, No. 02(0007)/11/EMR-II]. Crystallography was performed at the DST-FIST, India-funded Single Crystal Diffractometer Facility at the Department of Chemistry, University of Calcutta. We also acknowledge Center for Research in Nanoscience and Nanotechnology (CRNN), University of Calcutta for instrumental facilities.

References

1 S. Shylesh, V. Schünemann and W. R. Thiel, *Angew. Chem. Int. Ed.*, 2010, **49**, 3428.

2 (a) M. B. Gawande, A. K. Rathi, I. D. Nogueira, R. S. Varma and P. S. Branco, *Green Chem.*, 2013, **15**, 1895; (b) S. Pathak, K. Debnath, Md. M. R. Mollick and A. Pramanik, *RSC Adv.*, **2014**, *4*, 23779; (c) E. Kolvari, N. Koukabi and O. Armandpour, *Tetrahedron*, 2014, **70**, 1383.

3 (a) Multicomponent Reactions; Zhu, J., Bienaymé, H., Eds.; Wiley-VCH: Weinheim, 2005; For recent reviews, see: (b) A. Domling, *Chem. Rev.*, 2006, **106**, 17; (c) J. Zhu, *Eur. J. Org. Chem.*, 2003, **2003**, 1133; (d) D. J. Ramón and M. Yus, *Angew. Chem., Int. Ed.*, 2005, **44**, 1602; (e) C. Simon, T. Constantieux and J. Rodriguez, *Eur. J. Org. Chem.*, 2004, **2004**, 4957.

4 (a) G. J. T. Kuster, L. W. A. van Berkom, M. Kalmoua, A. van Loevezijn, L. A. J. M. Sliedregt, B. J. van Steen, C. G. Kruse, F. P. J. T. Rutjes and H. W. Scheeren, *J. Comb. Chem.*, 2006, **8**, 85; (b) C. Macleod, B. I. Martinez-Teipel, W. M. Barker, R. E. Dolle, *J. Comb. Chem.*, 2006, **8**, 132; (c) G. Lang, A. Pinkert, J. W. Blunt, M. H. G. Munro, *J. Nat. Prod*., 2005, **68**, 1796; (d) C. A. Maier and B. Wüensch, *J. Med. Chem.*, 2002, **45**, 438.

5 A. Fensome, W. R. Adams, A. L. Adams, T. J. Berrodin, J. Cohen, C. Huselton, A. Illenberger, J. C. Karen, M. A. Hudak, A. G. Marella, E. G. Melenski, C. C. McComas, C. A. Mugford, O. D. Slayeden, M. Yudt, J. Zhang, P. Zhang, Y. Zhu, R. C. Winneker and J. E. Wrobel, *J. Med. Chem.*, 2008, **51**, 1861.

6 G. Kumari, Nutan, M. Modi, S. K. Gupta and R. K. Singh, *Eur. J. Med. Chem.*, 2011, **46**, 1181.

7 K. Ding, Y. Lu, Z. Nikolovska-Coleska, S. Qiu, Y. Ding, W. Gao, J. Stuckey, K. Krajewski, P. P. Roller, Y. Tomita, D. A. Parrish, J. R. Deschamps, and S. Wang, *J. Am. Chem. Soc.* 2005, **127**, 10130.

8 V. V. Vintonyak, K. Warburg, H. Kruse, S. Grimme, K. Hubel, D. Rauth and H. Waldmann, *Angew. Chem., Int. Ed.*, 2010, **49**, 5902.

9 B. K. S. Yeung, B. Zou, M. Rottmann, S. B. Lakshminarayana, S. H. Ang, S. Y. Leong, J. Tan, J. Wong, S. Keller-Maerki, C. Fischli, A. Goh, E. K. Schmitt, P. Krastel, E. Francotte, K. Kuhen, D. Plouffe, K. Henson, T. Wagner, E. A. Winzeler, F. Petersen, R. Brun, V. Dartois, T. T. Diagana and T. H. Keller, *J. Med. Chem*., 2010, **53**, 5155.

10 K. Ding, Y. Lu, Z. Nikolovska-Coleska, G. Wang, S. Qiu, S. Shangary, W. Gao, D. Qin, J. Stuckey, K. Krajewski, P. P. Roller and S. Wang, *J. Med. Chem*., 2006, **49**, 3432.

11 (a) K. Debnath, S. Pathak and A. Pramanik, *Tetrahedron Lett.*, 2013, **54**, 896; (b) S. Pathak, K. Debnath and A. Pramanik, *Beilstein J. Org. Chem.*, 2013, **9**, 2344; (c) K. Debnath, S. Pathak and A. Pramanik, *Tetrahedron Lett.*, 2013, **54**, 4110; (d) K. Debnath, S. Pathak and A. Pramanik, *Tetrahedron Lett.*, 2014, **55**, 1743.

12 A. Mondal, M. Brown and C. Mukhopadhyay, *RSC Adv.*, 2014, **4**, 36890.

13 P. H. Yang, C. T. Qu and W. Z. Wang, *Res Chem Intermed*, 2013, **39**, 463.